CHAPTER 19

TIME-DEPENDENT QUASI-3D MODELING OF BREAKING WAVES ON BEACHES

Entin A. Karjadi[1] and Nobuhisa Kobayashi[2]

ABSTRACT: A time-dependent quasi-3D numerical model is developed to predict the temporal and cross-shore variations of the free surface elevation and fluid velocities in the surf and swash zones under obliquely incident waves. This model, which includes the dispersion due to the vertical variations of the instantaneous horizontal velocities, is an extension of the two-dimensional model of Kobayashi and Karjadi (1994, 1996). The developed model is compared with available laboratory and field data for planar beaches as well as field data for a barred beach. For planar beaches, the dispersion effects on the longshore current are significant for regular waves but secondary for irregular waves. For a barred beach, the model under the assumption of alongshore uniformity cannot predict the broad peak in the longshore current profile. The small alongshore variation of wave setup induced by a small alongshore variation of obliquely incident irregular waves is shown to significantly modify the driving force and longshore current profile in the bar trough region. On the other hand, for planar beaches, the alongshore current profile is shown to be insensitive to the small alongshore variation of obliquely incident waves. This may explain why existing longshore current models based on the assumption of alongshore uniformity were regarded to be adequate before their comparisons with the barred beach data.

INTRODUCTION

The time-averaged quasi-3D nearshore currents below the wave trough level have been modeled by various researchers (*e.g.*, DeVriend and Stive 1987; Svendsen and Lorenz 1989). These time-averaged models assume that the oscillatory wave motion is known, although no realistic model is available to predict the velocity field of breaking waves on beaches. Alternatively, a time-dependent quasi-3D numerical model, which runs on a workstation, is developed herein to predict the oscillatory and mean components of the 3D velocity field of obliquely incident breaking waves on beaches. This model is an extension of the time-dependent two-dimensional model of Kobayashi and Karjadi (1994, 1996) which is simply referred to as KK hereafter.

[1]Department of Civil Engineering, Bandung Institute of Technology, Jalan Ganesha 10, Bandung 40132, Indonesia. E-mail: entin@coastal.udel.edu

[2]Professor and Associate Director, Center for Applied Coastal Research, University of Delaware, Newark, DE 19716, USA. E-mail: nk@coastal.udel.edu

KK neglects the dispersion due to the vertical variations of the horizontal velocities although wave breaking produces vertical variations in the horizontal velocity and resulting energy dissipation. As a result, KK cannot reproduce the longshore current profile induced by regular waves breaking on planar beaches because it does not model the transition zone and lateral mixing. In this paper, KK is expanded to include the dispersion due to vertical variations of the horizontal velocities. Very little is known of the dispersion effects on surf zone hydrodynamics apart from the analysis of Svendsen and Putrevu (1994) that showed the importance of the dispersion effect due to the nonlinear interaction of cross-shore and longshore currents in explaining the measured cross-shore variations of long-shore currents induced by regular breaking waves. They used linear wave theory with depth-limited breaker height to describe the wave motion. The present analysis deals with the vertical variations of instantaneous horizontal velocities.

The dispersion terms due to the vertical variations of the horizontal velocities express additional cross-shore and alongshore momentum fluxes in the depth-integrated momentum equations. To predict these unknown momentum flux corrections, two new equations are derived from the corresponding three-dimensional shallow-water momentum equations using a method of moments. The quasi-3D model is compared with the same regular and irregular wave data for planar beaches as KK and with the field data of Smith *et al.* (1993) for a barred beach. The measurements of longshore currents on the barred beach during the DELILAH experiment generally indicated a broad peak in the bar trough region. Under the assumption of alongshore uniformity, the 3D model cannot explain this data. Low-frequency components and alongshore variations of incident irregular waves are examined to explain the broad peak of the longshore current. The longshore current profile on the barred beach is then shown to be sensitive to the alongshore variability unlike the longshore current profile on the planar beaches.

NUMERICAL MODEL

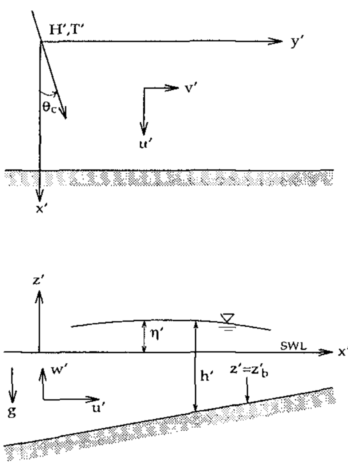

Figure 1: Definition sketch.

The approximate continuity and momentum equations used in this paper is derived from the three-dimensional continuity and Reynolds equations (Karjadi 1996) in a manner similar to the derivation for the two-dimensional case presented by Kobayashi and Wurjanto (1992). The symbol used in the derivation are depicted in Figure 1 where the prime indicates the physical variables that will be normalized later; x'=horizontal coordinate normal to the shoreline and positive landward; y' = horizontal coordinate parallel to the shoreline and positive in the downwave direction; z' = vertical coordinate and positive upward with z' = 0 at the still water level (SWL); z'_b=elevation of the seabed which is assumed to be impermeable and fixed; η' = free surface elevation above SWL; h'=total water depth given by $h' = (\eta' - z_b')$; u'=cross-shore velocity; v'=alongshore velocity; w' = vertical velocity; and g=gravitational acceleration. Limiting to waves in shallow water, the coordinates x', y', and z' are normalized by $\sigma H', \sigma H'/\theta_c$ and H', respectively, where $\sigma = T'\sqrt{g/H'}$, whereas T', H', and θ_c are the characteristic wave period, height and incident angle in radian used for the normalization.The corresponding fluid velocity components u', v', and w' in the x', y', and z' directions are normalized by $\sqrt{gH'}, \theta_c\sqrt{gH'}$ and H'/T', respectively. The normalized continuity and momentum equations are then simplified under the assumptions of $\sigma^2 \gg 1$ and $\theta_c^2 \ll 1$ for shallow water waves with small angles of incidence. The simplified equations are integrated from $z = z_b$ to $z = \eta$ using the kinematic boundary conditions at $z = z_b$ and η and the boundary conditions of zero tangential stresses at $z = \eta$. The derived continuity and horizontal momentum equations for $\sigma^2 \gg 1$ and $\theta_c^2 \ll 1$ are expressed in the following normalized forms (Kobayashi *et al.* 1997, Karjadi 1996)

$$\frac{\partial h}{\partial t} + \frac{\partial}{\partial x}(hU) = 0 \tag{1}$$

$$\frac{\partial}{\partial t}(hU) + \frac{\partial}{\partial x}\left(hU^2 + m\right) = -h\frac{\partial \eta}{\partial x} - \tau_{bx} \tag{2}$$

$$\frac{\partial}{\partial t}(hV) + \frac{\partial}{\partial x}(hUV + n) = -h\frac{\partial \eta}{\partial y} - \tau_{by} \tag{3}$$

with

$$m = \int_{z_b}^{\eta} (u - U)^2 \, dz \quad ; \quad n = \int_{z_b}^{\eta} (u - U)(v - V)\, dz \tag{4}$$

in which t = time, U = depth-averaged cross-shore velocity; V = depth-averaged alongshore velocity; τ_{bx} = cross-shore bottom shear stress; τ_{by} = alongshore bottom shear stress. The dispersion terms m and n defined in (4) express the cross-shore and alongshore momentum fluxes due to the vertical variations of u and v, respectively. The dispersion terms result from the vertical integration of the horizontal momentum equations.

The normalized variables without the primes in these equations are defined as

$$t = \frac{t'}{T'} \; ; \; x = \frac{x'}{\sigma H'} \; ; \; y = \frac{y'}{\sigma H'/\theta_c} \; ; \; z = \frac{z'}{H'} \; ; \; z_b = \frac{z_b'}{H'} \; ; \; \eta = \frac{\eta'}{H'} \tag{5}$$

$$h = \frac{h'}{H'} \; ; \; u = \frac{u'}{\sqrt{gH'}} \; ; \; v = \frac{v'}{\theta_c\sqrt{gH'}} \; ; \; U = \frac{U'}{\sqrt{gH'}} \; ; \; V = \frac{V'}{\theta_c\sqrt{gH'}} \tag{6}$$

$$\nu_t = \frac{\nu_t'}{H'^2/T'} \; ; \; \tau_{bx} = \frac{\tau_{bx}'}{\rho\sqrt{gH'}\,H'/T'} \; ; \; \tau_{by} = \frac{\tau_{by}'}{\rho\theta_c\sqrt{gH'}H'/T'} \; ; \; \sigma = \frac{T'\sqrt{gH'}}{H'} \tag{7}$$

in which ρ = fluid density; ν_t = normalized eddy viscosity used to express the turbulent stresses $\tau_x = \nu_t \partial u/\partial z$ and $\tau_y = \nu_t \partial v/\partial z$; and the parameter σ defined in (7) is the ratio of the cross-shore and vertical length scales. It is noted that the pressure is assumed to be approximately hydrostatic and the lateral turbulent stresses can be shown to be negligible for shallow-water breaking waves (Karjadi 1996).

For obliquely incident waves with $\theta_c^2 \ll 1$, the cross-shore fluid motion governed by (1) and (2) with $m = 0$ is the same as that for normally incident waves obtained by Kobayashi and Wurjanto (1992). Furthermore, the variations in the y-direction appear only in the term $\partial\eta/\partial y$ in (3) and along the seaward boundary of the computation domain.

In this model, the bottom boundary layer is not analyzed explicitly and the bottom stresses for $\theta_c^2 \ll 1$ are expressed as

$$\tau_{bx} = f_b|u_b|u_b \quad ; \quad \tau_{by} = f_b|u_b|v_b \quad ; \quad f_b = \frac{1}{2}\sigma f_b' \tag{8}$$

in which u_b and v_b are the cross-shore and alongshore velocities immediately outside the bottom boundary layer, respectively, and f_b' = bottom friction factor which is assumed constant. KK assumes that $m = 0$, $n = 0$, $u_b = U$ and $v_b = V$.

In this quasi-3D model, the equations for m and n are derived from the three-dimensional momentum equations using the algebraic procedure which may be called a method of moments. The resulting equations for m and n can be shown to be expressed as (Kobayashi *et al.* 1997, Karjadi 1996)

$$\frac{\partial m}{\partial t} + \frac{\partial}{\partial x}(3mU + m_3) = 2\left(U\frac{\partial m}{\partial x} - \tilde{u}_b\tau_{bx} - D_B\right) \tag{9}$$

$$\frac{\partial n}{\partial t} + \frac{\partial}{\partial x}(nU + mV + n_3) = V\frac{\partial m}{\partial x} - n\frac{\partial U}{\partial x} - \tilde{v}_b\tau_{bx} - \tilde{u}_b\tau_{by} - 2D_n \tag{10}$$

with

$$\tilde{u}_b = u_b - U \quad ; \quad \tilde{v}_b = v_b - V \tag{11}$$

$$m_3 = \int_{z_b}^{\eta} (u - U)^3\, dz \quad ; \quad n_3 = \int_{z_b}^{\eta} (u - U)^2 (v - V)\, dz \tag{12}$$

$$D_B = \int_{z_b}^{\eta} \nu_t \left(\frac{\partial u}{\partial z}\right)^2 dz \quad ; \quad D_n = \int_{z_b}^{\eta} \nu_t \frac{\partial u}{\partial z}\frac{\partial v}{\partial z} dz \tag{13}$$

The thickness of the bottom boundary layer is assumed to be much smaller than the water depth $h = (\eta - z_b)$, and the lower limit z_b of the integrations in (12) and (13) should be interpreted at the elevation immediately outside the bottom boundary layer. The contributions of the boundary layer flow, which needs to satisfy $u = 0$ at the bed, to the second moments m and n in (4) and the third moments m_3 and n_3 are assumed to be negligible. The normalized energy dissipation rate D_B due to the vertical variations of τ_x and u outside the boundary layer is the same as the dissipation rate due to breaking of normally incident waves used by Svendsen and Madsen (1984). The energy dissipation rate inside the bottom boundary layer corresponding to D_B is estimated as $u_b\tau_{bx}$ (Kobayashi and Wurjanto 1992) and is taken into account in (9). The boundary layer contribution corresponding to D_n is assumed to be given by $v_b\tau_{bx}$ and accounted for in (10) where $u_b\tau_{by} = v_b\tau_{bx}$ by use of (8).

To obtain h, U, V, m and n using (1)–(3), (9) and (10), u_b, v_b, m_3, n_3, D_B and D_n need to be expressed in terms of the five unknown variables. As a first attempt to deal with this closure problem, the horizontal velocities u and v outside the bottom boundary layer are assumed to be expressed as

$$u = U + \tilde{u}_b F(\zeta) \quad ; \quad v = V + \tilde{v}_b F(\zeta) \quad ; \quad \zeta = (z - z_b)/h \tag{14}$$

in which F is assumed to be a function of ζ only with $\zeta = 0$ at the bottom and $\zeta = 1$ at the free surface. The definitions of $\tilde{u}_b$ and $\tilde{v}_b$ in (11) require $F = 1$ at $\zeta = 0$. Furthermore, the turbulent eddy viscosity ν_t' is assumed to be given by $\nu_t' = (C_\ell h')^2 \, |\partial u'/\partial z'|$ outside the bottom boundary layer where the turbulence measurements by Cox *et al.* (1994) indicate that the mixing length parameter C_ℓ is on the order of 0.1. Accordingly, the normalized eddy viscosity ν_t is expressed as

$$\nu_t = \sigma C_\ell^2 h^2 \left| \frac{\partial u}{\partial z} \right| \tag{15}$$

Substitution of (14) and (15) into (4), (12) and (13) yields

$$m = C_2 h \tilde{u}_b^2 \quad ; \quad n = C_2 h \tilde{u}_b \tilde{v}_b \quad ; \quad C_2 = \int_0^1 F^2 d\zeta \tag{16}$$

$$m_3 = C_3 h \tilde{u}_b^3 \quad ; \quad n_3 = C_3 h \tilde{u}_b^2 \tilde{v}_b \quad ; \quad C_3 = \int_0^1 F^3 d\zeta \tag{17}$$

$$D_B = C_B \sigma C_\ell^2 \mid \tilde{u}_b \mid^3 ; \quad D_n = C_B \sigma C_\ell^2 \mid \tilde{u}_b \mid \tilde{u}_b \tilde{v}_b ; \quad C_B = \int_0^1 \mid \frac{dF}{d\zeta} \mid^3 d\zeta \tag{18}$$

in which the constants C_2, C_3 and C_B can be found for the specified functional form of F. To find $\tilde{u}_b$ using $m = C_2 h \tilde{u}_b^2$ for given $h \geq 0$ and $m \geq 0$, it is assumed that $\tilde{u}_b \leq 0$ for $U \geq 0$ and $\tilde{u}_b > 0$ for $U < 0$ to ensure $|u_b| \leq |U|$ where $u_b = (U + \tilde{u}_b)$ is the near-bottom cross-shore velocity used in (8). After $\tilde{u}_b$ is obtained, $\tilde{v}_b = n/(C_2 h \tilde{u}_b)$, $v_b = (V + \tilde{v}_b)$, and (17) and (18) yield m_3, n_3, D_B and D_n.

Finally, the function F needs to be specified. Svendsen and Madsen (1984) assumed a cubic profile for their analysis of a single turbulent bore on a beach. For regular and irregular breaking waves on beaches, the following cubic profile is tentatively assumed:

$$F = 1 - (3 + 0.75a)\,\zeta^2 + a\zeta^3 \qquad \text{for} \quad 0 \leq \zeta \leq 1 \tag{19}$$

in which a = cubic velocity profile parameter. Comparison of (19) and the cubic profile assumed by Svendsen and Madsen (1984) suggests that a is about 3. The shear stresses at the surface are zero only if $a = 4$. For the range a = 3–4, F is not very sensitive to a, C_2 = 0.49–0.55, C_3 = -0.07–0.00, and C_B = 12.3–15.2 (Johnson *et al.* 1996). The computed results using C_ℓ = 0.1–0.2 in (15) and a = 3–4 in (19) are found to be very similar. The typical values of $C_\ell = 0.1$ and $a = 3$ are hence employed for the computed results presented in this paper.

The numerical method used in the quasi-3D model is an extension of the numerical method devised in KK to solve (1)–(3) with $m = 0$ and $n = 0$. The computer program developed for the quasi-3D model solves (1)–(3), (9) and (10) along with (8), (11) and (16)–(18) using the MacCormack method (MacCormack 1969). The procedure is described in detail in Karjadi (1996).

COMPARISON WITH AVAILABLE DATA

1 Comparison with Laboratory and Field Data for Planar Beaches

The comparisons of the 2D model of KK and and the quasi-3D model with the laboratory experiments 2–5 of Visser (1991) and the field data of Thornton and Guza (1986) on February 5 and 6, 1980 are presented in Kobayashi *et al.*

(1997). The 3D computations are made in the same way as the corresponding 2D computations presented in KK. For regular waves, the dispersion term n in the alongshore momentum equation (3) definitely improves the prediction of the cross-shore variation of longshore current. The bottom friction factor f_b' in (8) is adjusted somewhat for experiments 4 and 5 to obtain better agreement. The alongshore bottom shear stress τ_{by} in (3) is important in determining the magnitude of $\overline{V}$ but modifies its profile little as expected from the previous work (*e.g.*, Longuet-Higgins 1970).

For irregular waves, the dispersion term n improves the agreement somewhat if the bottom friction factor f_b' is reduced to $f_b' = 0.01$ from $f_b' = 0.015$ used for the 2D model. Moreover, the dispersion effects on the longshore currents induced by breaking irregular waves are secondary in comparison to breaking regular waves. To confirm this conclusion, the time-averaged alongshore momentum equation corresponding to (3) is expressed as

$$\frac{\partial}{\partial x} S_{xy} + \frac{\partial \overline{n}}{\partial x} + \overline{h}\frac{\partial \overline{\eta}}{\partial y} + \frac{1}{2}\frac{\partial}{\partial y}\overline{(\eta - \overline{\eta})^2} = \overline{\tau}_{by} \tag{20}$$

in which $S_{xy} = \overline{hUV}$ is the alongshore radiation stress based on U and V. The third and fourth terms in (20) are zero for the case of alongshore uniformity. The computed cross-shore variations of dS_{xy}/dx and $d\overline{n}/dx$ for regular and irregular waves are presented in Kobayashi *et al.* (1997). For regular waves, the term $d\overline{n}/dx$ included in the 3D model decreases the force driving the longshore current near the breaker point but increases this force near the shoreline. On the other hand, for irregular waves the term $d\overline{n}/dx$ is secondary in the alongshore momentum equation (20).

2 Comparison with Field Data for A Barred Beach

On a barred beach, conceptually, waves will break on the bar, reform and break again on the beach face producing two peaks in the longshore current distribution. Contrary to this concept, the measurements of longshore currents on a barred beach obtained during the DELILAH experiment (Smith *et al.* 1993) generally indicated a broad peak in the bar trough region. Existing time-averaged models for longshore currents, which couple four governing equations for the wave height, wave angle, mean water surface elevation, and longshore current, have not been able to predict these broad peak longshore current data (Smith *et al.* 1993).

Smith *et al.* (1993) developed a one-dimensional time-averaged numerical model for longshore current that included the effect of turbulence due to wave breaking through a general transport equation for the mean turbulent kinetic energy. Their model produced an unrealistic high peak on the beach face. Church and Thornton (1993) developed a model using a spatially varying bottom friction coefficient based on a one-dimensional turbulent kinetic energy equation associated with the breaking-wave induced turbulence. However, this model was unable to satisfactorily predict the broad peak of the longshore current distribution observed in the DELILAH experiment. Momentum fluxes associated with mass transport above the trough level of broken waves, which were ignored in the other models, were included in the model developed by Kuriyama (1994). His model with additional empirical coefficients was compared with field data in Japan. At present, there is no model available to predict the broad peak of the longshore current on a barred beach in a physically satisfactory manner.

To assess whether the developed model including the dispersion effects is capable of predicting the longshore current on a barred beach, the 3D model is compared with the DELILAH field data of Smith *et al.* (1993) on October 14, 1990 at 1900 EST which included the cross-shore variations of the measured root-mean-square wave height and longshore current. The frequency spectrum measured at the 8 m water depth was narrow banded in frequency with symmetric directional distributions about a mean oblique wave direction. The wave conditions at the 8 m depth were: the root-mean-square wave height $H'_{\rm rms} = 0.83$ m; the spectral peak period $T'_p = 12.0$ sec; and the dominant incident wave direction $\theta_i = 18°$. The bathymetry was nearly uniform in the alongshore direction.

The seaward boundary of the numerical model based on the assumption of shallow water waves is taken at the water depth $d' = 3.64$ m below the still water level where the measured root-mean-square wave height $H'_{\rm rms}$ was 1.02 m. The measured frequency spectrum at $d' = 8$ m is used to estimate the assumed unidirectional frequency spectrum and the predominant incident wave direction at $d' = 3.64$ m using the computer program RESHOAL developed by Poff and Kobayashi (1993) as explained briefly in the following.

RESHOAL assumes a straight shoreline with parallel bottom contours. For a given incident directional random wave spectrum at a deeper water depth, RESHOAL computes the directional random wave spectrum at a specified shallow water depth using linear finite-depth wave theory for directional random wave shoaling and refraction (LeMéhauté and Wang 1982). The incident directional random wave spectrum at the deeper water depth $d' = 8$ m is assumed to be given by the product of the TMA frequency spectrum and the Mitsuyasu-type directional spreading function. The input parameters for RESHOAL at the deeper water depth $d' = 8$ m are: $H'_{\rm mo}$ = spectral estimate of significant wave height; T'_p = spectral peak period ($T'_p = 12$ s for this data); γ = spectral peak enhancement factor; θ_i = dominant incident wave direction ($\theta_i = 18°$); $s_{\max}$ = maximum value of the spreading parameter. RESHOAL computes the directional spectrum, frequency spectrum and directional spreading function at the shallower water depth $d' = 3.64$ m. The parameters $H'_{\rm mo}$, γ, and $s_{\max}$ need to be calibrated such that the root-mean-square of wave height at the 3.64 m depth is equal to the measured value of $H'_{\rm rms}$ =1.02 m and the assumed incident directional wave spectrum at the 8 m water depth is similar to the measured spectrum. The calibrated values are $H'_{\rm mo} = 1.35$ m; γ =5; and $s_{\max}$=120 at the 8 m water as shown in Figure 2. It is noted that the assumption of $H'_{\rm rms} = H'_{\rm mo}/\sqrt{2}$ yields $H'_{\rm rms} = 0.95$ m for $H'_{\rm mo} = 1.35$ m, which is slighty larger than the measured value $H'_{\rm rms} = 0.83$ m. This might indicate wind effects on wind waves between the 8 m and 3.64 m water depths.

Figure 2 shows the measured and fitted frequency and directional spectra at the 8 m water depth and the computed frequency and directional spectra at the seaward boundary $d' =$ 3.64 m. The fitted directional spectrum at the 8 m depth is the TMA frequency spectrum with $\gamma = 5$ and $H'_{\rm mo} = 1.35$ m with the Mitsuyasu-type directional spreading function with $s_{\max} = 120$. The computed frequency spectrum with $T'_p = 11.9$ s at $d' = 3.64$ m is used to compute the incident wave trains at the seaward boundary required as the input to the 3D model. This incident frequency wave spectrum does not include low-frequency wave components as shown in Figure 2. The computed dominant incident wave direction is $\theta_i = 12°$ at $d' = 3.64$ m as may be seen from the computed directional spectrum at $d' = 3.64$ m in Figure 2 which suggests that the assumption of unidirectional random waves may be reasonable.

Similar to the computations made in KK, the normalized computation duration is taken as $t_{\max} = 500$ corresponding to $t'_{\max} \simeq 99$ min. The sampling rate $\Delta t'_s$ is taken to be the same as the sampling rate of the field data, $\Delta t'_s = 0.125$ s. The bottom friction factor is assumed to be $f'_b = 0.015$. The computed results presented in the following are based on the normalization using the wave conditions at the seaward boundary of $d' = 3.64$ m, *i.e.*, the measured root-mean-square wave height $H' = H'_{\mathrm{rms}} = 1.02$ m; the computed spectral peak period $T' = T'_p = 11.9$ sec; and the computed dominant wave direction $\theta_i = 12°$. Correspondingly, $\sigma = T'(g/H')^{\frac{1}{2}} = 37$ and $\theta_c = \theta_i = 0.21$ in radians. The assumptions of $\sigma^2 \gg 1$ and $\theta_c^2 \ll 1$ are satisfied for this data. The normalized grid spacings are taken as $\Delta x \simeq \Delta y = 0.0106$ corresponding to the dimensional cross-shore and alongshore grid spacings of $\Delta x' = 0.40$ m and $\Delta y' = 1.91$ m, respectively.

Figure 3, with the parameter $\delta_\eta = 0$ for the case of uniform incident wave conditions in the alongshore direction, shows the comparisons between the measured and computed cross-shore variations of the local root-mean-square wave height H_{rms} and the longshore current $\overline{V}$ together with the measured bottom profile. The computed temporal variation of η for $200 \leq t \leq 500$ is used to obtain H_{rms} based on the zero-up crossing method whereas the computed longshore current $\overline{V}$ is obtained by averaging the temporal variation of the depth-averaged alongshore velocity V for the duration $200 \leq t \leq 500$. Figure 3 with $\delta_\eta = 0$ shows that the 3D model without the incident low-frequency wave components underpredicts the root-mean-square wave height in the bar trough region. Moreover, the model predicts a peak in the longshore current at the seaward edge of the bar crest in contrast to a broad peak in the bar trough region.

As a first attempt to explain the broad peak in the longshore current distribution, the effects of incident low-frequency waves on the cross-shore distribution of longshore current are examined because incident low-frequency waves might modify the wave breaking on the bar crest and resulting longshore current profile. The incident wave spectrum at the seaward boundary shown in Figure 2 does not include low-frequency components. As a first approximation, uniform low-frequency components are added to the incident wave spectrum to examine the effects of these low-frequency components to the longshore current profile. The additional low-frequency components are found to modify the longshore current profile little (Karjadi 1996). Consequently, the broad peak of the longshore current in the bar trough cannot be explained by incident low-frequency waves.

The effect of alongshore non-uniformity on the longshore current profile is examined in the following. Longshore currents have been primarily modeled assuming alongshore uniformity, although it has been known that alongshore non-uniformities affect longshore currents (*e.g.*, Putrevu *et al.* 1995). To study the effect of the alongshore variation of incident wave conditions within the limitation of the 3D model based on three cross-shore lines as discussed in KK,

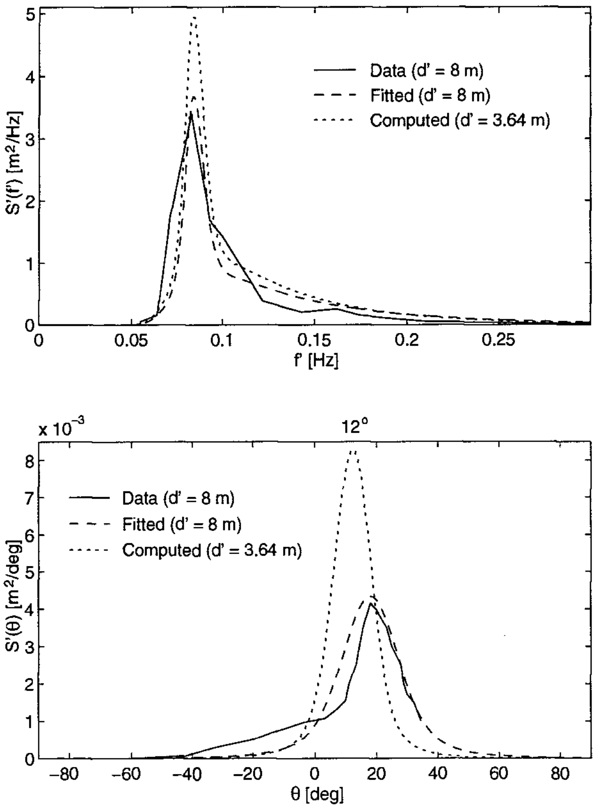

Figure 2: Measured and fitted frequency and directional spectra at depth $d' = 8$ m and the shoaled and refracted frequency and directional spectra at $d' = 3.64$ m.

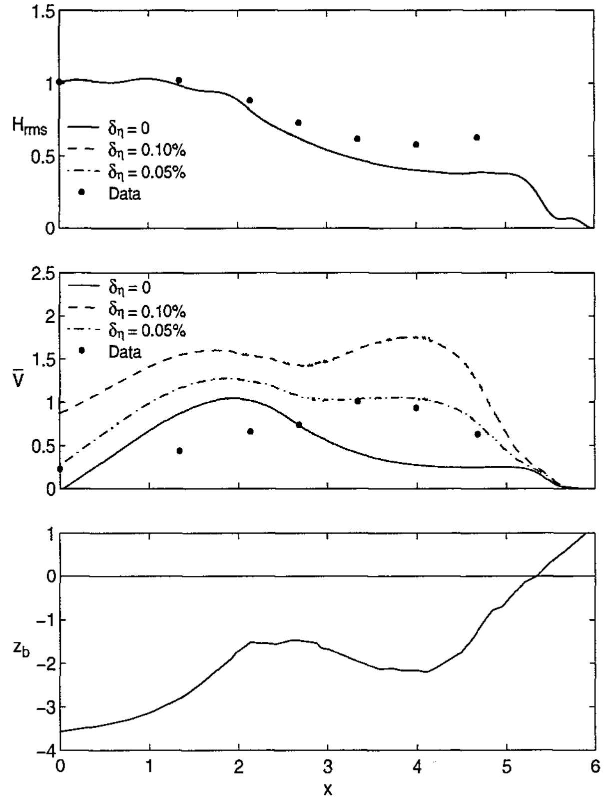

Figure 3: Measured and computed cross-shore variations of $H_{\rm rms}$ and longshore current $\overline{V}$ together with normalized bottom profile for DELILAH experiment with $\delta_\eta \geq 0$.

the incident wave trains η_i specified as new input to the model are modified as follows:

$$\begin{aligned} \text{Line 1:}\quad \text{new } (\eta_i)_1 &= \text{old } (\eta_i)_1 \\ \text{Line 2:}\quad \text{new } (\eta_i)_2 &= \text{old } (\eta_i)_2 \times (1-\delta_\eta) \\ \text{Line 3:}\quad \text{new } (\eta_i)_3 &= \text{old } (\eta_i)_3 \times (1-2\,\delta_\eta) \end{aligned}$$

where the old time series $(\eta_i)_1, (\eta_i)_2$ and $(\eta_i)_3$ have been computed for incident unidirectional random waves of alongshore uniformity. The distance between two adjacent lines is $\Delta y' = 1.91$ m. The dimensionless parameter δ_η is taken to be much less than unity to satisfy the assumption of gradual alongshore variation. The incident wave intensity decreases or increases in the down-wave direction depending on $\delta_\eta > 0$ or $\delta_\eta < 0$, respectively.

The computed results using these new incident wave trains are shown in Figures 3 and 4 for the cases of $\delta_\eta = 0$, 0.0005 and 0.001 and for the cases of $\delta_\eta = 0$ and -0.001, respectively. The root-mean-square wave height changes very little since the specified change in the incident wave train is very small. For the wave intensity decreasing in the down-wave direction, the longshore current profile increases almost uniformly across the shoaling region and over the bar crest. The increase in the longshore current is larger in the bar trough region, whereas the increase is smaller in the swash zone. The broad peak in the bar trough region in Figure 3 is similar to the broad peak observed in the field. For the wave intensity increasing in the down-wave direction as shown in Figure 4 the longshore current in the bar trough region is decreased significantly and becomes negative.

To explain the computed results shown in Figures 3 and 4, Figure 5 shows the cross-shore variations of the driving forces on the left hand side of (20) for the cases of $\delta_\eta = 0.001$ and -0.001. The terms of $\partial\overline{n}/\partial x$ and $\frac{1}{2}\partial\overline{(\eta-\overline{\eta})^2}/\partial y$ are on the order of 0.005 or less in the bar trough region and secondary in comparison to the other two terms plotted in these figures. For both cases, the cross-shore gradient of the alongshore radiation stress, $\partial S_{xy}/\partial x$, driving the longshore current is very small in the bar trough region. The additional term $\overline{h}\partial\overline{\eta}/\partial y$ associated with the alongshore wave setup gradient modifies the driving force significantly in the bar trough region where the incident wave intensity and resulting wave setup decrease or increase in the down-wave direction depending on $\delta_\eta > 0$ or $\delta_\eta < 0$, respectively.

To examine the effects of the alongshore non-uniformity on planar beaches, the modified incident wave trains for the cases of $\delta_\eta = 0.0005$ and 0.001 are also specified for the computations for the regular wave experiment 2 of Visser (1991) and the irregular wave data of Thornton and Guza (1986) on February 5. For the planar beaches as shown in Figure 6, the longshore current increases almost uniformly in the shoaling and surf zones except in the swash zone. Contrary to the computed results for the barred beach shown in Figure 3, the longshore current profile shape on the planar beaches is not sensitive to the alongshore non-uniformity. To explain this difference, Figure 7 shows the cross-shore variations of the driving forces in the time-averaged momentum equation (20) for the regular and irregular waves on the planar beaches. The additional driving force terms $\overline{h}\partial\overline{\eta}/\partial y$ and $\frac{1}{2}\partial\overline{(\eta-\overline{\eta})^2}/\partial y$ due to the alongshore variations are small

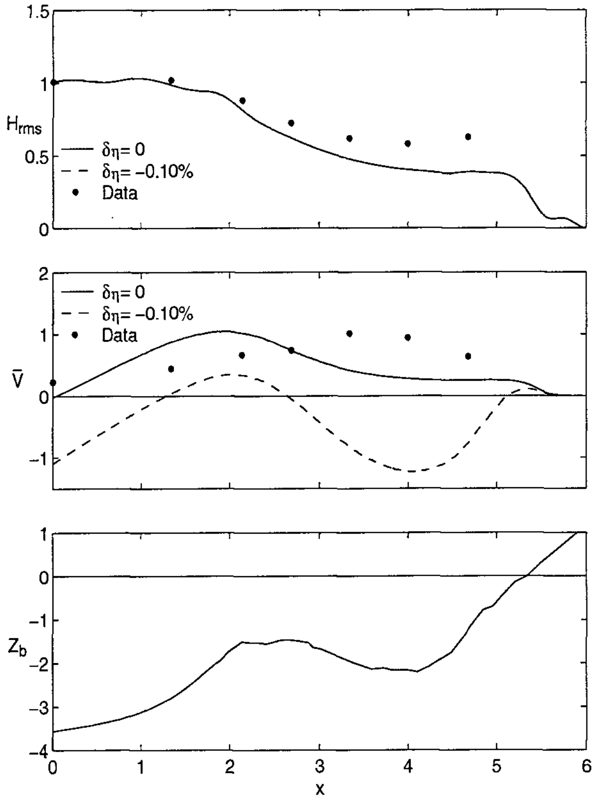

Figure 4: Measured and computed cross-shore variations of $H_{\rm rms}$ and longshore current $\overline{V}$ together with normalized bottom profile for DELILAH experiment with $\delta_\eta \leq 0$.

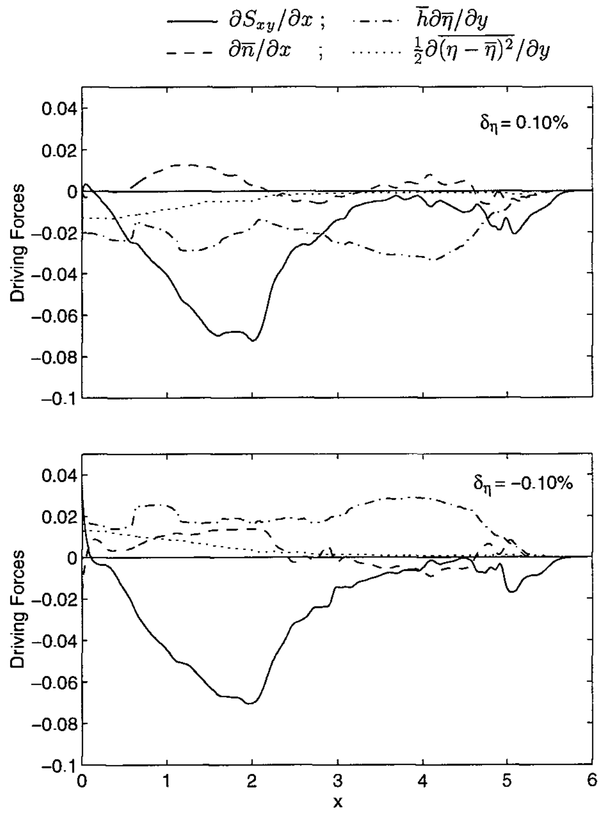

Figure 5: Computed cross-shore variations of driving forces in time-averaged alongshore momentum equation (20) for a barred beach.

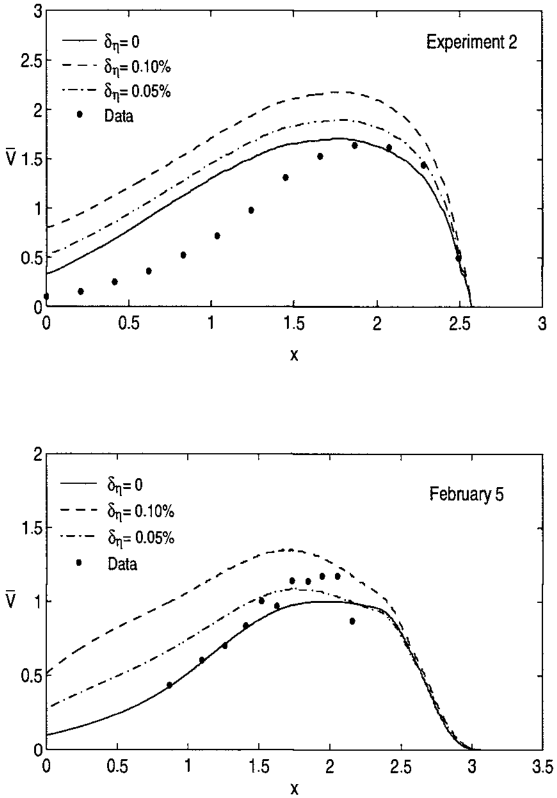

Figure 6: Effects of alongshore decrease of incident wave intensity on the longshore current profile for planar beaches.

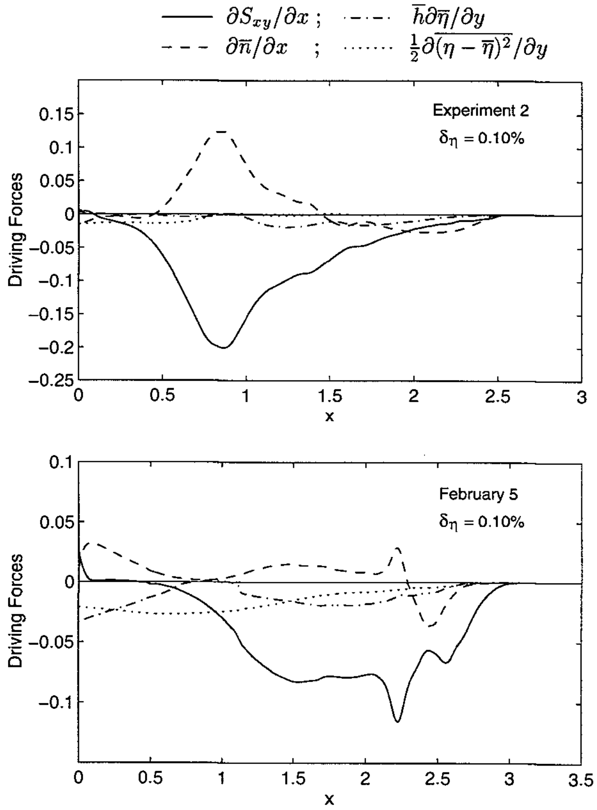

Figure 7: Computed cross-shore variations of driving forces in time-averaged alongshore momentum equation (20) for planar beaches.

in comparison to the main driving force, $\partial S_{xy}/\partial x$, causing the almost uniform increase in the longshore current without changing its shape as shown in Figure 6. It is noted that the term $\partial \overline{n}/\partial x$ in (20) is important for regular waves as discussed in relation to (20).

The computed results discussed above imply that the broad peak of the longshore current on a barred beach can be caused by the very small alongshore variation of wave height and setup. This may explain why existing longshore current models based on the assumption of alongshore uniformity were regarded to be adequate before their comparisons with the barred beach data. For planar beaches, the effect of alongshore non-uniformity, even if it exists, can be accounted for by adjusting the constant bottom friction factor which changes the longshore current profile shape little. On the other hand, for barred beaches, the very small alongshore variation of wave height and setup modifies the longshore current profile shape which cannot be changed much by adjusting the constant bottom friction factor.

CONCLUSIONS

A time-dependent quasi three-dimensional numerical model is developed to predict the temporal and cross-shore variations of the free surface elevation and fluid velocities in the surf and swash zones under obliquely incident waves. This model is used to clarify the dispersion effects due to the vertical variation of the horizontal velocities in the surf zone. For planar beaches, the dispersion effects on the cross-shore variations of the wave height and setup are shown to be minor, indicating that the cross-shore dispersion term m may be neglected in the depth-integrated cross-shore momentum equation (2) as anticipated by Kobayashi and Wurjanto (1992). On the other hand, the dispersion effects on the longshore current profile are significant for regular waves but secondary for irregular waves, especially in view of the uncertainties associated with the bottom friction factor.

The 3D model is also compared with the DELILAH field data for a barred beach (Smith *et al.* 1993). Under the assumption of alongshore uniformity, the model cannot explain the observed broad peak in the longshore current in the bar trough region. Small alongshore variations of the incident wave intensity and resulting wave setup are shown to modify the longshore current profile in the bar trough region significantly. The cross-shore gradient of the alongshore radiation stress driving the longshore current is very small in this bar trough region. The alongshore gradient of wave setup is shown to alter the force driving the longshore current significantly in this region and produces a broad peak in the longshore current. Contrary to the computed results for the barred beach, the longshore current profile on planar beaches is found to be insensitive to the alongshore variations of the incident wave intensity and resulting wave setup. As a result, the prediction of the longshore current profiles on barred beaches will require the knowledge of small alongshore variability that is very difficult to measure accurately.

ACKNOWLEDGMENT

This work was supported by the U.S. Army Research Office, University Research Initiative under Contract No. DAAL03-92-G- 0116, by the NOAA Office of Sea Grant, Department of Commerce, under Grant No. NA85AA-D-SG033 (Project SG95 R/OE-18), and by the National Science Foundation under Grant No. CTS-9407827.

REFERENCES

Church, J.C. and Thornton, E.B., 1993. "Effects of breaking wave induced turbulence within a longshore current model." *Coast. Engrg*, **20**, 1–28.

Cox, D.T., Kobayashi, N. and Okayasu, A. (1994). "Vertical variations of fluid velocities and shear stress in surf zones." *Proc. 24th Coast. Engrg. Conf.*, ASCE, **1**, 98–112.

DeVriend, H.J. and Stive, M.J.F. (1987). "Quasi-3D modelling of nearshore currents." *Coast. Engrg.*, **11**, 565–601.

Johnson, B.D., Kobayashi, N. and Cox, D.T. (1996). "Formulation and validation of vertically two-dimensional shallow-water wave model." *Proc. 25th Coast. Engrg. Conf.*, ASCE (in press).

Karjadi, E.A. (1996). "Numerical models for obliquely incident waves in surf and swash zones." Ph.D. dissertation, Univ. of Delaware, Newark, Del.

Kobayashi, N. and Karjadi, E.A. (1994). "Swash dynamics under obliquely incident waves." *Proc. 24th Coast. Engrg. Conf.*, ASCE, **2**, 2155–2169.

Kobayashi, N. and Karjadi, E.A. (1996). "Obliquely incident irregular waves in surf and swash zones." *J. Geophys. Res.*, **101**(C3), 6527–6542.

Kobayashi, N. and Karjadi, E.A., and Johnson, B.D. (1997). "Dispersion effects on longshore currents in surf zones." *J. Wtrwy, Port, Coast. and Oc. Engrg.*, ASCE (in press).

Kobayashi, N. and Wurjanto, A., 1992. "Irregular wave setup and run-up on beaches." *J. Wtrwy, Port, Coast. and Oc. Engrg.*, ASCE, **118**(4), 368–386.

Kuriyama, Y., 1994. "Numerical model for longshore current distribution on a bar-trough beach." *Proc. 24th Coast. Engrg. Conf.*, ASCE, **2**, 2237–2251.

LeMéhauté, B. and Wang, J.D., 1982. "Wave spectrum changes on a sloped beach." *J. Wtrwy, Port, Coast. and Oc. Engrg*, ASCE, **108**(1), 33–47.

Longuet-Higgins, M.S., 1970. "Longshore currents generated by obliquely incident sea waves, 1 and 2." *J. Geophys. Res.*, **75**(C3), 6778-6801.

MacCormack, R.W., 1969. "The effects of viscosity in hypervelocity impact cratering." *Paper 69-354*, American Institute of Aeronautics and Astronautics, New York.

Poff, M.T. and Kobayashi, N., 1993. "Computer program for refraction of directional random waves." *Res. Rept. No. CACR-93-04*, Ctr. for Applied Coast. Res., Univ. of Delaware, Newark, DE.

Putrevu, U., Oltman-Shay, J. and Svendsen, I.A., 1995. "Effect of alongshore nonuniformities on longshore current predictions." *J. Geophys. Res.*, **100**(C8), 16119–16130.

Smith, J,M., Larson, M. and Kraus, N.C. (1993). "Longshore current on a barred beach: field measurements and calculation." *J. Geophys. Res.*, **98**(C12), 22727–22731.

Svendsen, I.A. and Lorenz, R.S. (1989). "Velocities in combined undertow and longshore currents." *Coast. Engrg.*, **13**, 55–79.

Svendsen, I.A. and Madsen, P.A., 1984. "A turbulent bore on a beach." *J. Fluid Mech.*, **148**, 73–96.

Svendsen, I.A. and Putrevu, U., 1994. "Nearshore mixing and dispersion" *Proc. Roy. Soc. London*, A(445), 561–576.

Thornton, E.B. and Guza, R.T. (1986). "Surf zone longshore currents and random waves: Field data and models." *J. Phys. Oceanogr.*, **16**, 1165–1178.

Visser, P.J. (1991). "Laboratory measurements of uniform longshore currents." *Coast. Engrg.*, **15**, 563–593.